Published in
Gradient Index, Miniature, and Diffractive Optical Systems II - Proceedings of SPIE 4437, 134-141, 2001
which should be used for any reference to this work

Efficient beamshaping of high-power diode-lasers using micro-optics

H. P. Herzig[a], A. Schilling[a], L. Stauffer[b], U. Vokinger[b], M. Rossi[c]

[a]Institute of Microtechnology, University of Neuchatel, Rue A.-L. Breguet 2, CH-2000 Neuchatel
[b]Leica Geosystems AG, CH-9435 Heerbrugg
[c]Heptagon, Zurich Office, Badenerstrasse 569, CH-8048 Zurich

ABSTRACT

We designed, fabricated and characterized a micro-optical beamshaping device, intended to optimize the coupling of an incoherent, linearly extended high-power diode-laser into a multimode fiber. The device uses two aligned micro-optical elements (DOEs) in combination with conventional optics. With a first prototype we achieved an overall efficiency of 28 %. Straightforward improvements, like antireflective coatings and the use of graytone elements, should lead to an efficiency of about 50 %. The device is compact and the fabrication is suited for mass production at low cost. We applied three different technologies for the fabrication of the micro-optical elements and compared the performance. The technologies were: direct laser writing, multiple projection photolithography in combination with reactive ion etching (RIE) in fused silica, and high-energy-beam-sensitive (HEBS) glass graytone lithography in photoresist. We found that the refractive type elements (graytone) yield better efficiency for large deflection angles, while diffractive elements give intrinsically accurate deflection angles.

1. INTRODUCTION

High-power, pulsed diode-lasers are used in rangefinder systems for distance measurements. For these rangefinders the achievable measurement range depends directly on available laser output power. In turn, the available laser output power per unit length is limited by the damage threshold of the material. Therefore, more output power results in a larger active region and the geometrical shape of the emitting surface is typically a line. Efficient collimation of such a partially coherent, linearly extended light source with large divergence angles is a non-trivial problem and difficult to achieve with conventional optics. We designed, fabricated, and characterized a micro-optical device with two aligned diffractive or refractive optical elements in combination with conventional [1]. The goal was to achieve a high coupling efficiency of such a linear diode-laser into a multimode fiber, using a compact and low cost optical system that is suited for mass fabrication. The diode-laser was coupled into a multimode fiber to simplify the quantification of the performance. In the final rangefinder application, the transformed light distribution is imaged onto the distant object. Leger and Goltsos [2] used a similar concept as described here to convert a mutually incoherent linear diode-laser array into a 2-dimensional source with maximum radiance and symmetrized shape and divergence. Their system was designed to optimize end pumping of solid-state lasers.

2. WORKING PRINCIPLE

While the diode-laser is fully coherent perpendicular ("$\perp$") to the line-shaped active region, the spatial coherence extends only to a fraction of the total length in the parallel direction ("$\parallel$") (x-axis in Figs. 1 and 2). Therefore, a coherent beamshaping element, as for example designed by an iterative Fourier algorithm,[3,4] or a coherent addition with a fan-in element,[5] are not appropriate approaches for the beamshaping problem which is addressed here. The special coherence properties of the source necessitate an incoherent beamshaping method.

The main characteristic of a diode-laser is the emitting wavelength λ, the lateral extension of the active region $d_\perp$ and $d_\parallel$, and the numerical apertures $NA_\perp = \sin\theta_\perp$ and $NA_\parallel = \sin\theta_\parallel$. $\theta_\perp$ and $\theta_\parallel$ are the corresponding divergence half angles. The employed diode-laser had a wavelength of λ = 850 nm, lateral extensions of $d_\perp$ = 1 µm and $d_\parallel$ = 350 µm, and measured numerical apertures of $NA_\perp$ = 0.51 and $NA_\parallel$ = 0.12. The 1-D space bandwidth product (SBP) of a light source is defined as [6]

$$SBP = (d/\lambda)\, NA \tag{1}$$

where d and NA are the lateral dimension and the numerical aperture, respectively. For a diffraction limited Gaussian beam the space bandwidth product is [7]

$$SBP = 2/\pi. \tag{2}$$

The SBP of the high-power diode-laser is therefore practically diffraction limited in the direction perpendicular to the active region, and typically a factor of 50 larger than the diffraction limited case in the parallel direction. The main problem for the beamshaping of the linear, edge emitting diode-laser lies in the fact that with conventional optics the SBP in one direction stays constant at best. Only the ratio between the NA and d can be changed. The basic principle of our beamshaping device is to symmetrize the lateral dimensions and the NA of the emitting source such that $SBP_{\perp} = SBP_{\parallel}$ with $SBP_{\perp} \cdot SBP_{\parallel} = \text{const}$. For that purpose, the line source is divided into three equal parts and redistributed on the fiber with the desired values for the NA and the lateral extensions. Consequently, we increase the coupling efficiency into the fiber and correspondingly enlarge the measurement range for rangefinders, because of the increased intensity on the target. Within the wave propagation model, which was used for the theoretical description of the system, we modeled the linear diode-laser as an incoherent superposition of 75 independent Gaussian sources with beam waists corresponding to the measured divergence angles. The division of the source is achieved with the first micro-optical element. Ideally this should be done directly in the source plane, but since the fast axis collimation has to be done first, the various mutually incoherent Gaussian beams begin to overlap in the direction parallel to the emitting edge. This causes a small efficiency loss, which is approximately proportional to the overlap region between neighboring incoherent Gaussian beams, and therefore approximately proportional to the distance between the active region of the source and the first diffractive optical element (DOE).

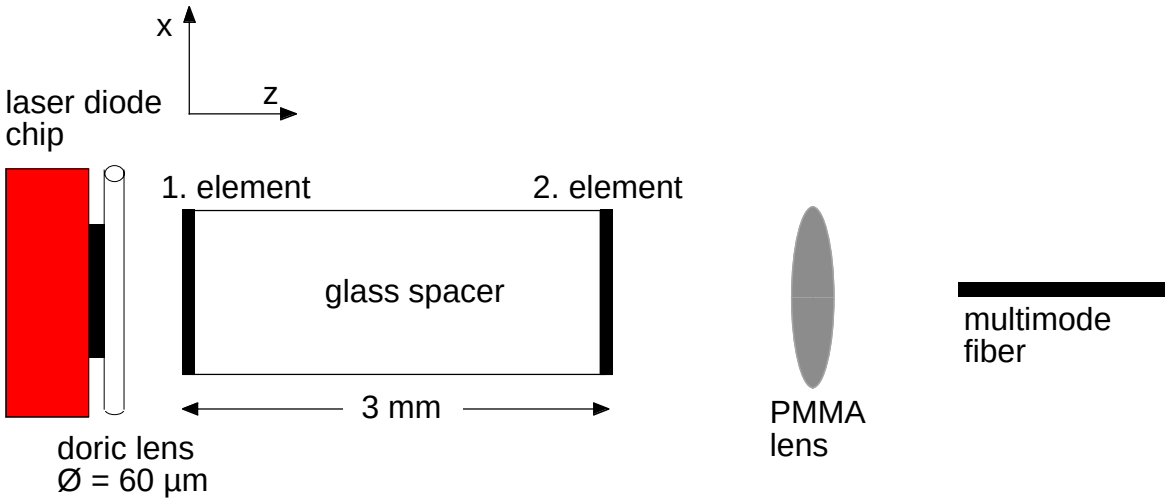

Fig. 1: Schematic optical setup with the diode-laser chip (active region: 1 µm x 350 µm), the combined micro-optical element, an additional Polymethyl-Methacrylate (PMMA) imaging lens, and the optical multimode fiber (∅ = 100 µm, NA = 0.2).

3. THE OPTICAL SETUP

The complete optical setup is schematically displayed in Fig. 1. The fast and slow NA of the diode-laser were measured to be $NA_{\perp} = 0.51$ and $NA_{\parallel} = 0.12$, respectively. A cylindrical gradient-index lens (Doric Lenses Inc., Canada), which had a specified effective numerical aperture of NA = 0.5 and a diameter of 60 µm, was mounted directly after the active region in order to collimate the fast axis. Since the tolerances for mounting the gradient-index lens are very tight, it was aligned manually, using

micrometer stages, by measuring the far field intensity distribution, and finally glued onto the laser chip. The theoretical NA after the Doric lens was $NA_{\perp} = 0.0083$. Subsequently, the beamshaping device follows, which is composed of two DOEs with a glass spacer in between. The first DOE, with a size of 370 μm x 370 μm, divides the line source into three equal parts along the x-axis and directs them into three different directions. The working principle is schematically shown in Fig. 2. In parts 1 and 3 of the first DOE there are three different optical functions implemented: a prism function perpendicular, a prism function parallel, and a focusing function parallel to the emitting edge of the diode-laser. The central part 2 has only the focusing function, which collimates the beam parallel to the active region. The second DOE, with a size of 800 μm x 800 μm, redirects the parts 1 and 3 of the intensity distribution in the direction parallel to the emitting edge. The final conventional Polymethyl-Methacrylate (PMMA) lens after the second DOE has two optical functions. It creates a reduced image of the transformed source at the fiber plane, and at the same time serves to superpose the three parts of the source onto each other. The multimode fiber has a diameter of 100 μm with a numerical aperture of NA = 0.2.

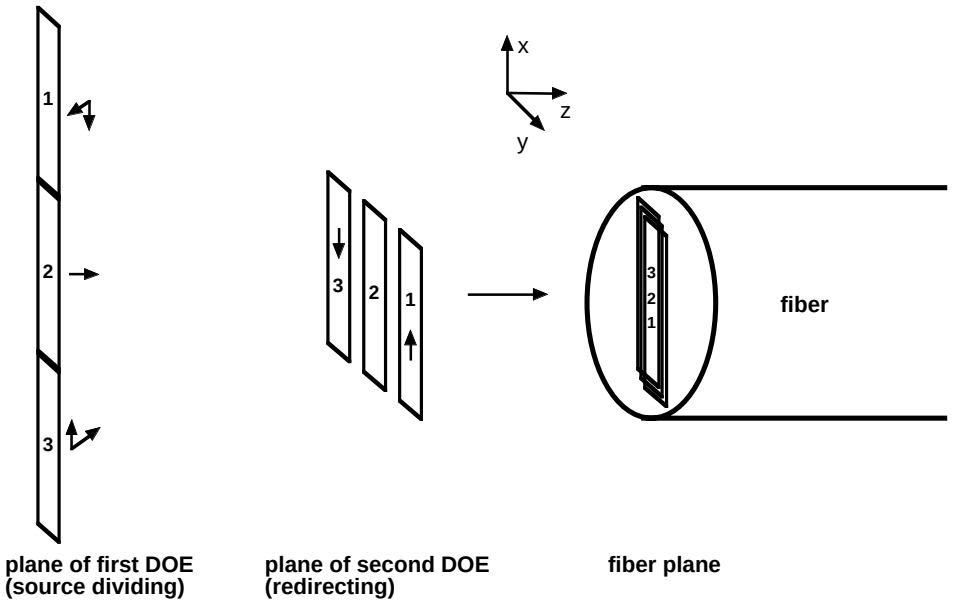

Fig. 2: Schematic working principle of the beamshaping device (the Doric and the PMMA lens are omitted for clarity). The different parts of the source are denoted by the numbers 1, 2, and 3. The arrows mark the prism functions in the planes of the two DOEs.

4. RESULTS AND DISCUSSION

The two DOEs were fabricated by direct laser writing [8,9] in photoresist with the laser writer at CSEM in Zurich, Switzerland. Since the elements are quite small, a large number of elements can be written on one wafer. Subsequent replication and mounting procedure are also wafer compatible, so that parallel fabrication technology can be used until the dicing of the combined DOEs. Therefore, the fabrication, alignment and mounting process is suited for mass fabrication at low cost.

The diffraction efficiency of the two DOEs was characterized before mounting, using focused light from a VCSEL with a wavelength of 850 nm. The first element had an averaged efficiency of 74 %, the second element of 87 %. The two DOEs and the borofloat glass spacer with a thickness of 600 μm were then aligned and glued together with UV curable lens bond optical cement, using a Karl Suss maskaligner MA/BA6. The alignment marks were written by the laser writer at the same time as the DOEs. The alignment of the two DOEs with respect to each other was better than 5 μm. The total thickness of the combined DOE after mounting was 3 mm (Fig. 5).

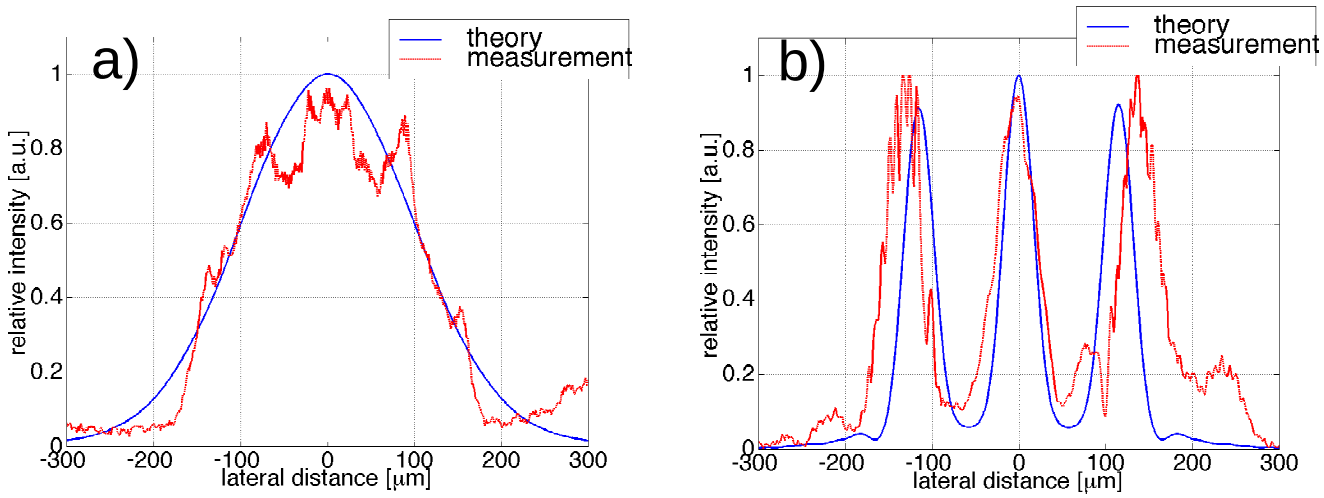

Fig. 3: Calculated and measured intensity distributions in the plane of the second DOE: (a) cross section parallel to the slow axis of the diode-laser, (b) cross section parallel to the fast axis of the diode-laser.

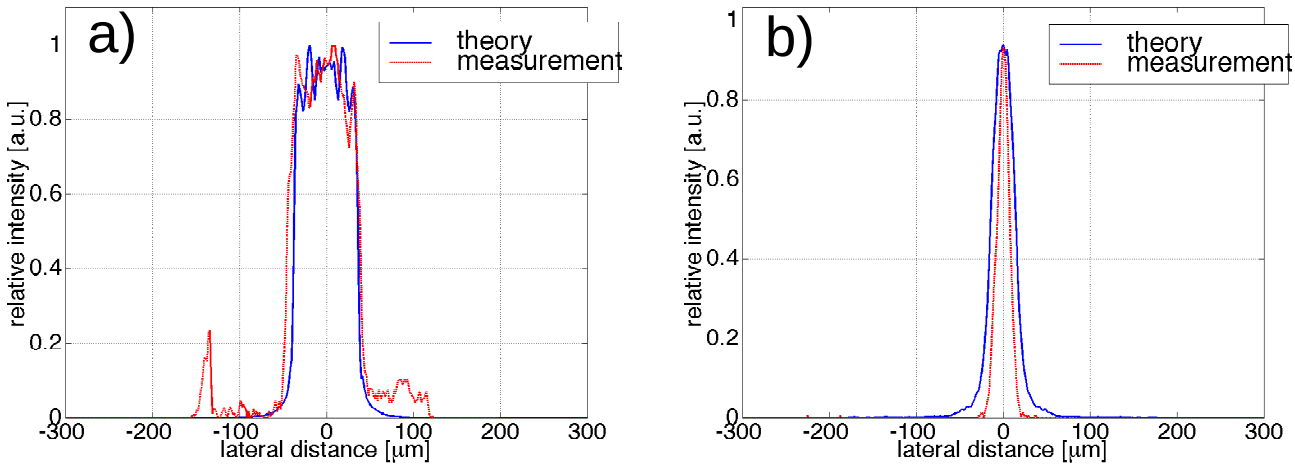

Fig. 4: Calculated and measured intensity distributions in the plane of the fiber: (a) cross section parallel to the slow axis of the diode-laser, (b) cross section parallel to the fast axis of the diode-laser.

For the theoretical optimization of the system design we used the commercially available raytrace program Code V^{TM}. The performance of the final setup was then analyzed quantitatively with a wave propagation model using different propagation methods as described in detail in reference [7]. Diffraction at apertures is fully taken into account within this model, and Fresnel losses at the optical surfaces can be considered in an approximate way. For the comparison of theoretical and experimental intensity distributions we used the wave propagation model, where we modeled the linear diode-laser by an incoherent superposition of 75 independent Gaussian sources with beam waists corresponding to the measured divergence angles. Calculated and measured intensity cross sections in the plane of the second DOE and in the fiber plane are shown in Figs. 3 and 4, respectively. The agreement between the theoretical and experimental intensity distributions is very satisfying. A possible

cause for the observed small differences could be the non-uniformity of the emitted intensity at the active region of the diode-laser, and the possibly limited accuracy of the description of the source by the incoherent superposition of Gaussian beams.

Table 1: Experimental efficiencies and estimated optimization potential considering antireflection coatings and micro-optical elements fabricated by laser writing. The efficiency and the optimization potential refer to the overall efficiency.

position	experimental efficiency	optimization potential between subsequent positions
laser output	100 %	n. a.
after GRIN lens	80 %	5 %
after 1th DOE	48 %	8 %
after 2nd DOE	38 %	2 %
fiber	28 %	7 %

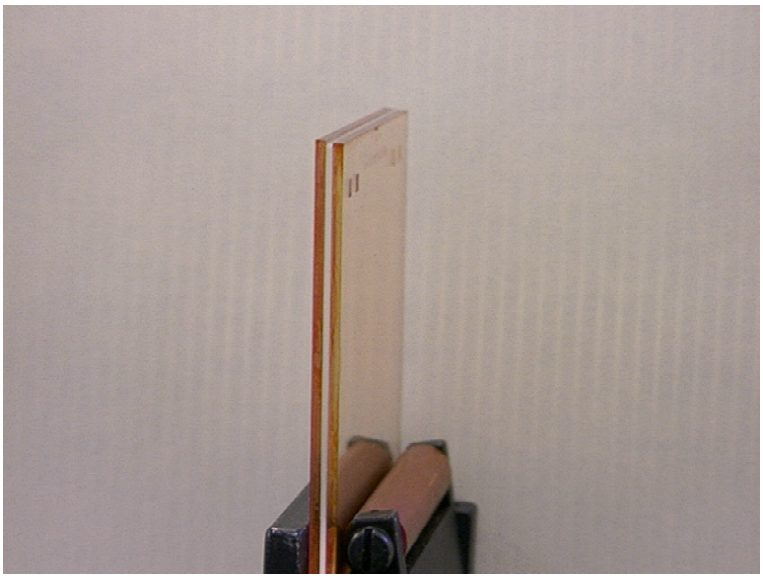

Fig. 5: Two diffractive elements (resist) with a glass spacer in between.

We measured a value of about 80 % for the collimating efficiency of the gradient-index lens. With the wave propagation model we obtained a value of about 88 %, taking into account Fresnel losses. Concerning the theoretical value, a 4 % loss originates from diffraction effects at the aperture, while another 8 % are Fresnel losses. The overall efficiency of the beamshaping device is given by the ratio of the light power coupled into the fiber divided by the emitted laser power. For the overall efficiency we obtained experimentally 28 %. The theoretical value is 80 %, assuming ideal DOEs and no Fresnel losses. The difference between theoretical and experimental values has two main reasons. First, there are Fresnel losses which account in total to about 14 %. These losses can be eliminated by antireflection coatings on all optical surfaces. Second, the non-ideal DOEs result in an overall efficiency loss of about 27 %. The DOEs, especially the first element with the smaller grating periods, can be replaced by refractive type elements with increased efficiency fabricated by HEBS glass graytone technology. A comparison of different technologies for the fabrication of the two micro-optical elements is given in Section 5. An efficiency increase of about 10 % for the first element is realistic, which would result in about 50 % overall efficiency for an optimized device including antireflection coatings. The reason for the fundamental losses are mainly twofold: coupling losses for the collimation of the fast angle by the gradient-index lens, which amount to about 4 %, and overlap losses of about 5 % which originate from the fact that certain coherent source points hit two different parts of the first DOE. This second loss is limited by the minimum distance between the

diode-laser and the first micro-optical element, about 100 µm, and is mainly determined by the gradient-index lens with the smallest available diameter of 60 µm. The other 11 % are due to diffraction effects at the apertures of the system. Table 1 summarizes the experimentally determined efficiencies together with the estimated optimization potential.

Since the NA of the impinging light at the fiber plane is important for the coupling efficiency, we measured the NA for the fast and the slow axis in the fiber plane and calculated the corresponding values with the wave propagation model. We obtained for the slow axis an experimental value of NA = 0.12 compared to a theoretical value of NA = 0.16. For the fast axis we obtained experimentally NA = 0.09 and theoretically NA = 0.11. The experimental and theoretical values for the fast axis agree reasonably well, while for the slow axis the experimental value is significantly smaller. A possible reason for the difference between experimental and theoretical values for the slow axis could lie in the simplified description of the diode-laser as a superposition of incoherent Gaussian sources within the wave propagation model.

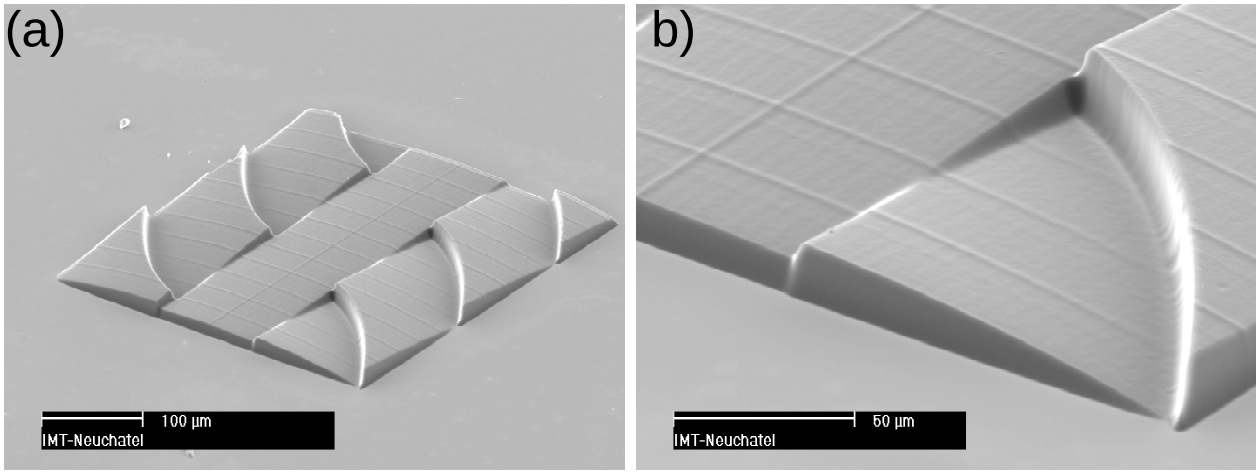

Fig. 6: SEM image of the first element fabricated by HEBS glass graytone lithography in photoresist: (a) overview, (b) enlarged detail.

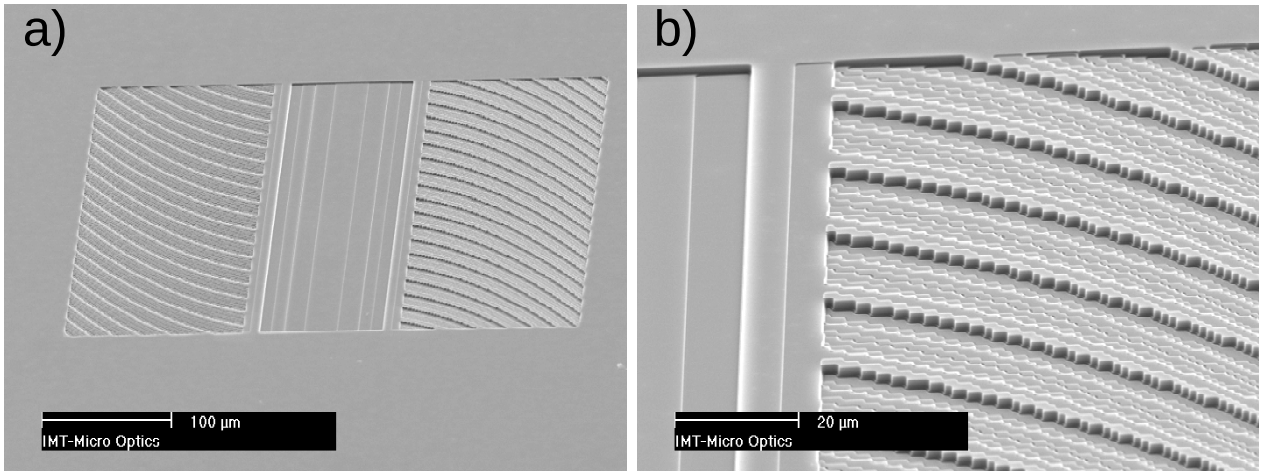

Fig. 7: EM image of the first element fabricated as multilevel structure(8 levels) in fused silica: (a) overview, (b) enlarged detail.

5. COMPARISON OF DIFFERENT FABRICATION TECHNOLOGIES

Besides direct laser beam writing in photoresist,[8,9] we also used two other technologies for the fabrication of the two micro-optical elements of the beamshaping device: binary mask photolithography in combination with reactive ion etching,[11] resulting in 8-level fused silica elements, and High-Energy-Beam-Sensitive (HEBS) glass graytone lithography in photoresist,[10,12,13] resulting in deep continuous surface-relief structures. We compare the performance of the different fabrication technologies with respect to the two micro-optical elements, which were used for the beamshaping device, and discuss the different sources of loss.

The laser written elements are in photoresist and were realized as continuous diffractive surface relief profile with a depth of 2.8 μm, designed for the second order. Since the HEBS-glass graytone technology (as well as the laser writing) offers the possibility to fabricate continuous relief elements with a large profile depth (15-20 μm), the elements can also be realized with much less zone transitions. In the example described here, the elements were realized as continuous refractive surface profile with a depth of 18 μm. The elements fabricated by graytone lithography in photoresist are shown in Fig 6. The 8-level fused silica elements have a diffractive surface profile with a depth of 1.65 μm. As a consequence of the relatively small grating periods of the first element compared to the minimum feature size of 1.25 μm, the effective number of phase levels was partially smaller than 8. The first element fabricated by binary mask technology as 8-level element in fused silica is shown in Fig. 7. One can clearly see the three different parts of each of the elements with the different optical functions implemented.

Two main characteristics are of importance for the performance of the two micro-optical elements in the beamshaping device: the accuracy of the deflection angles under which the light is deviated, and the efficiency of the deflection into this direction. Therefore, we analyzed the efficiency and the deflection angles of the elements fabricated by the three technologies. The efficiencies were measured with the focused light from a VCSEL diode at the design wavelength λ = 850 nm. The spot size (full width at $1/e^2$ intensity level) in the plane of the element was measured with a knife edge to be 50 μm. We found that the efficiencies of the second element achieved with the three different technologies were nearly equal, slightly above 80 %. For the first element, which has steeper slopes and correspondingly smaller grating periods, the graytone element had a higher efficiency (79 % and 85 %), while the laser written elements and the multilevel elements performed nearly equal (74 %). For the graytone elements the lower one of the two efficiencies includes the losses at the non-ideal profile steps, whereas the higher efficiency (purely refractive) is measured when the beam does not hit such a step. The sources of the loss for the different elements are quite different. For the multilevel elements the losses are mainly due to the approximation of the ideal profile by the multilevel structure and the alignment errors between the different lithographic steps. For the laser written elements, the main losses are caused by the finite width of the writing beam and surface roughness. The main losses of the graytone elements are due to the surface roughness and the non-ideal profile steps.

Interesting is also the comparison of the measured and designed deflection angles of the two elements, which were fabricated by the different technologies. The multilevel elements reproduced nearly exactly the designed deflection angles (< 1 %), the laser written elements showed slight deviations from the design values (< 2.5 %), while the differences were largest for the graytone elements (< 10 %). For the multilevel elements the directions are determined by the grating periods. For the refractive graytone elements the directions are determined by the surface profile, which is more difficult to control for the deep elements studied here.

For the diffractive elements, as fabricated by laser writing and multiple projection lithography, we translated the difference between measured and designed deflection angles into the corresponding grating period deviation. For the multilevel elements the corresponding grating period deviation was about 60 to 90 nm for elements A and B, respectively. This is about 5-7 % of the minimum feature size (mfs), and a reasonable value for the accuracy of the e-beam writing of the chromium mask. For the laser written elements we found corresponding grating period deviations of about 220 to 280 nm for elements A and B, respectively. The pixel size used for the raster scan during exposure was 400 nm, and the grating period deviations therefore correspond to about half the pixel size, which is also a reasonable value.

6. CONCLUSIONS

We designed, fabricated and characterized a micro-optical incoherent beamshaping device, intended to optimize the coupling of a linear high-power diode-laser into a multimode fiber. We achieved an overall efficiency of 28 % with a first prototype, which corresponds well to the theoretical values obtained with a wave propagation model. Straightforward improvements, like antireflective coatings and the use of graytone elements, should lead to an efficiency of about 50 %. The beamshaping device is compact and the fabrication is well suited for mass production at low cost. Used in a rangefinder measurement system, this micro-optical device will extend the measurement range because of the symmetrized intensity distribution obtained on a distant target.

We compared three different technologies for the fabrication of the two micro-optical elements of the beamshaping device. Refractive type elements (graytone) yield better efficiency for large deflection angles, while diffractive elements (multilevel or laser written) give intrinsically accurate deflection angles.

ACKNOWLEDGMENTS

This research was supported by the Swiss Priority Program OPTIQUE II. The authors would like to thank the CSEM in Neuchatel, Switzerland, for the fabrication of the multilevel gratings in fused silica, and Dr. Kley, Friedrich-Schiller-Universitat Jena, Germany, for the e-beam writing of the HEBS glass mask. We also would like to thank Irene Philipoussis, IMT Neuchatel, Christian Ossmann and Dr. Stefan Seider, Karl Suss AG, Munchen, and Dr. Michael Scheidt for technical help.

REFERENCES

[1] B. Gachter, A. Schilling, L. Stauffer, U. Vokinger, "Optischer Entfernungsmesser," *European Patent Application* 00108836.8 (2000), patent pending.

[2] J. R. Leger, W. C. Goltsos, "Geometrical transformation of linear diode-laser arrays for longitudinal pumping of solid state lasers," IEEE J. Quantum Electron. 28, 1088-1100 (1992).

[3] J.N. Mait, "Understanding diffractive optic design in the scalar domain," *J. Opt. Soc. Am. A* **12**, 2145-2158 (1995).

[4] C. Kopp, L. Ravel, P. Meyrueis, "Efficient beamshaper homogenizer design combining diffractive optical elements, microlens array and random phase plate," *J. Opt. A: Pure Appl. Opt.* **1**, 398-403 (1999).

[5] P. Ehbets, H.P. Herzig, R. D\"andliker, P. Regnault, and I. Kjelberg, "Beam shaping of high-power laser diode arrays by continuous surface-relief elements," *J. Mod. Opt.* **40**, 637-645 (1993).

[6] J.W. Goodmann, *Introduction to Fourier Optics*, McGraw-Hill International (1996).

[7] U. Vokinger, *Propagation, Modification and Analysis of Partial Coherent Light Fields*, Ph.D. Thesis Universit de Neuchatel (1999).

[8] M.T. Gale, M. Rossi, "Continuous-relief diffractive lenses and microlens arrays," *in Diffractive Optics for Industrial and Commercial Applications*, J. Turunen, F. Wyrowsky, eds., (Akademie Verlag Berlin, 1997).

[9] M.T. Gale, Th. Hessler, R.E. Kunz, H. Teichmann, "Fabrication of continuous-relief micro-optics: progress in laser writing and replication technology," *OSA Technical Digest Series* **5**, 335 (1996).

[10] Ch. Gimkiewicz, D. Hagedorn, J. Jahns, E.-B. Kley, F. Thoma, "Fabrication of microprisms for planar optical interconnections by use of analog gray-scale lithography with High-Energy-Beam-Sensitive Glass," *Appl. Opt*. **38**, 2986-2990 (1999).

[11] M.B. Stern, "Binary Optics Fabrication," in *Micro-Optics: Elements, Systems, and Applications*, H.P. Herzig, ed. (Taylor & Francis, London, 1997).

[12] C. Wu, "Method of making high energy beam sensitive glass," U.S. patent 5,078,771 (1992).

[13] W. Daschner, C. Wu, S.H. Lee, "General aspheric refractive micro-optics fabricated by optical lithography using a high energy beam sensitive glass gray-level mask," *J. Vac. Sci. Technol. B* **14**, 135-138 (1996).